

DOI: <https://doi.org/10.15276/hait.07.2024.22>

UDC 004.662.99·519.6

Quality control of functioning of the structure “object-thermoelectric cooler-heat sink” of the system of providing thermal modes

Vladimir P. Zaykov¹⁾ORCID: <https://orcid.org/0000-0002-4078-3519>; gradan@i.ua. Scopus Author ID: 57192640250Vladimir I. Mescheryakov²⁾ORCID: <https://orcid.org/0000-0003-0499-827X>; gradan@ua.fm. Scopus Author ID: 57192640885Andriy S. Ustenko²⁾ORCID: <https://orcid.org/0000-0002-0546-7019>; uas059877@gmail.comAnastasiya S. Troynina³⁾ORCID: <https://orcid.org/0000-0001-6862-1266>; anastasiyatroynina@gmail.com. Scopus Author ID: 57193992712¹⁾ Research Institute STORM, 27, Tereshkova Str. Odessa, 65076, Ukraine²⁾ Odesa Mechnikov National University, 2, Dvoryanska Str. Odessa, 65082, Ukraine³⁾ Odesa Polytechnic National University, 1, Shevchenko Ave. Odessa, 65044, Ukraine

ABSTRACT

The analysis of the mathematical model of the system of providing thermal modes with the use of thermoelectric cooling to assess the influence of the conditions of heat exchange of the heat sink with the medium on the main parameters, reliability indicators and dynamic characteristics of a single-cascade thermoelectric cooler at a given temperature level of cooling, medium temperature, geometry of branches of thermoelements for different current operating modes is considered. The results of calculations of the main significant parameters, reliability indicators, dynamic and energy characteristics of a single-cascade cooler and heat sink of the selected design at a given temperature level of cooling, medium temperature, thermal load, geometry of branches of thermoelements for various characteristic current operating modes are given, when the conditions of heat exchange on the heat sink of the given design under variation of the heat transfer coefficient. It is shown that with the increase of air flow velocity on the heat sink the heat transfer coefficient increases and thus the temperature drop on the heat sink of the thermoelectric cooler with the medium decreases, which allows to significantly reduce the relative failure rate of the cooler and thus increase the probability of failure-free operation of the whole device. When operating a system for providing thermal modes comprising a cooling device, a heat sink, and an electric fan used for dissipating heat output to the environment, different modes of operation of the electric fan (air flow rate) can be used. With the increase in air flow rate of the electric fan increases the velocity of air flow in the live section of the heat sink of a given design, which leads to an increase in the heat transfer coefficient. This, in turn, makes it possible to reduce the temperature drop at a given design of the system for ensuring thermal modes. The possibility of control of reliability indicators, namely, relative intensity of failures and probability of failure-free operation of thermal mode systems of different designs (current modes, number of thermocouples, surface area of the heat sink) at a given cooling level (medium temperature, thermal load, geometry of thermocouples) under changing conditions of heat exchange of the heat sink with the medium is considered.

Key words: Reliability indicators; dynamic characteristics; mass and dimensions; temperature difference; current mode

For citation: Zaykov V. P., Mescheryakov V. I., Ustenko A.S., Troynina A. S. “Quality control of functioning of the structure “object - thermoelectric cooler - heat sink” of the system of providing thermal modes”. *Herald of Advanced Information Technology*. 2024; Vol. 7 No.3: 309-320. DOI: <https://doi.org/10.15276/hait.07.2024.22>

INTRODUCTION

The main function of the system of ensuring thermal modes (SETM) is to increase reliability indices of heat-loaded elements of radio-electronic equipment. The heat-removable element is practically in the same heat-loaded conditions as the critical element, and the connecting link of heat flow transfer to the environment affects the mass and size characteristics of the system. From the point of view

of reliability indicators and dynamics of SETM the main significant heat-loaded element is the thermoelectric cooler (TEC), because the control component of the regulator is usually located in more favorable temperature conditions. The TEC as an actuator of the supply system is an active device that generates a temperature differential at an electrode that is in contact with the heat loaded element. Temperature control in the contact area is a necessary control function, so the presence of a temperature sensor is mandatory. Comparing the inertia of the temperature sensor and thermoelectric

© Zaykov V., Mescheryakov V., Ustenko A., Troynina A. 2024

This is an open access article under the CC BY license (<https://creativecommons.org/licenses/by/4.0/deed.uk>)

cooler the time constant of the sensor can be neglected the delay in the formation of the primary thermal field, which is the primary information for control. The simplest way to solve the problem is the inverse filtering of the temperature field realized on the TEC. The method is acceptable for a limited number of distributed heat-loaded elements with coolers connected through heat pipes or directly to radiators of heat flow discharge to the external environment. It is obvious that the components of the system ‘object-TEC-radiator’ have mutual influence and should be considered in a complex and needs to be investigated.

LITERATURE REVIEW

The requirements to reliability and mass-size characteristics of systems for ensuring thermal modes of electronic equipment are constantly increasing [1]. Comparative analysis with other types of heat extraction systems shows the advantages of the thermoelectric method in terms of reliability, dynamics, mass-size characteristics [2, 3]. Existing automatic control systems are divided into groups with one input and one output SISO and systems with many inputs and many outputs MIMO [4, 5]. Localized systems are used in case of independent control of actuators, which is possible when their number is limited or there are no requirements to mass and dimensional characteristics [6, 7]. However, the issues of reliability of functioning of such systems have not been properly developed, since the reliability indicators are determined by parametric indicators determined by a specific type of the used element base [8]. The most promising coolers for the task at hand are thermoelectric devices [9, 10]. At the same time, the ever-increasing requirements for the growth of reliability indices and reduction of mass and dimensional characteristics force to search for ways to improve the quality of the actuator [11]. Theoretical and experimental studies of thermoelectric actuators are presented in [12], the influence of mechanical parameters on the main indicators of reliability and energy are given in [13], thermoelectric materials [14]. The stress state of a thermoelectric cooler has a significant impact on reliability indices and is used in accelerated tests [15], which should be taken into account in fast-acting SETMs [16]. The relationship between reliability performance and dynamics of TECs has been investigated in [17], and the influence of limited power consumption in [18]. At the same

time, the above studies considered separate components of the SETM, in particular, the thermoelectric cooler. The influence of the cooling object, the TEC and the heat sink were considered independently, which does not correspond to the real state of affairs and represents an actual research problem.

PURPOSE AND OBJECTIVES OF THE STUDY

The purpose of this work is to improve the reliability of the structure ‘object-TEC-radiator’ thermoelectric system of providing thermal modes of heat-loaded equipment.

To achieve this goal it is necessary to solve the following tasks:

- 1) to analyze the model of thermoelectric cooler and radiator of heat flow discharge into the surrounding space;
- 2) to analyze the management of reliability indicators of the complex ‘object-TEC-radiator’.

ANALYSES OF THE MODELS OF THERMOELECTRIC AND HEAT SINK

Let's use the mathematical model [18] to obtain the results of connection of the main parameters and indicators of thermoelectric system of providing temperature modes. The results of calculations of the main indicators of reliability, dynamic and energy characteristics of the SETM system with the use of a single-cascade TEC under the variation of conditions of heat exchange of the heat sink with the medium at the temperature level of cooling $T_0 = 260\text{K}$, $T_c = 300\text{K}$, thermal load $Q_0 = 2.0\text{ W}$, geometry of branches of thermoelements (ratio $l/S = 10$) for various characteristic current operating modes are shown in Table 1. Here: T_c is ambient temperature; Θ is relative temperature difference; B is relative operating current; I is operating current value; W – power consumption; E is refrigeration coefficient; U is voltage drop on the TEC; $\frac{Q_0}{n}$ is thermal load on one thermocouple; τ is time to reach the stationary mode; N is amount of given energy; αF is heat dissipation capacity of the radiator; α is heat transfer coefficient; λ/λ_0 is relative failure rate; P is probability of failure-free operation; n is number of thermocouples; F is area of the radiator.

Table 1. Results of calculations of the main significant parameters in modes

1 – Q_{0max} , 2 – $(nI)_{min}$, 3 – $(nI \lambda/\lambda_0 \tau)_{min}$, 4 – λ_{min}

M	T	Θ	B	I	W	E	U	$\frac{Q_0}{n}$	τ	N	αF	α	λ ₁ /λ ₂	λ/λ ₀	λ · 10 ⁸	P
<i>n</i> =20.5 pcs <i>F</i> =490 sm ²																
1	310	0.62	1.0	5.0	12.6	0.16	2.5	0.0973	9.0	113	1.46	30	1.0	21	63.0	0.9937
	307	0.59	0.82	4.1	8.6	0.23	2.1	0.0977	9.0	77	1.51	31	2.1	9.8	29.4	0.9971
	305	0.56	0.77	3.8	7.5	0.27	2.0	0.0977	9.0	66	1.9	39	2.8	7.4	22.4	0.9978
	303	0.54	0.73	3.6	6.7	0.30	1.9	0.0976	8.7	59	2.9	60	3.5	6.0	18	0.9982
	302	0.52	0.70	3.5	6.3	0.32	1.9	0.0976	8.6	54	4.15	85	4.1	5.1	15.4	0.9985
	300	0.50	0.66	3.3	5.6	0.32	1.7	0.0975	8.4	47	-	-	5.3	4.0	12.0	0.9988
<i>n</i> =23.3 pcs <i>F</i> =380 sm ²																
2	310	0.62	0.79	3.9	9.3	0.22	2.4	0.084	10.2	95	1.13	30	1.0	9.6	29	0.9971
	307	0.59	0.72	3.6	7.6	0.27	2.1	0.086	9.94	75	1.37	36	1.45	6.6	19.8	0.9980
	305	0.56	0.68	3.4	6.9	0.29	2.0	0.086	9.96	68	1.76	47	1.85	5.2	15.5	0.9984
	303	0.54	0.65	3.26	6.2	0.31	1.9	0.086	9.6	60	2.76	73	2.2	4.4	13.2	0.9987
	302	0.52	0.63	3.17	5.9	0.34	1.8	0.086	9.4	56	4.0	105	2.5	3.8	11.5	0.9989
	300	0.50	0.60	3.0	5.3	0.38	1.8	0.086	9.2	49	-	-	3.2	3.0	9.0	0.9991
<i>n</i> =30.3 pcs <i>F</i> =350 sm ²																
3	310	0.62	0.65	3.3	8.6	0.23	2.6	0.066	104	1.06	30	1.0	5.8	33.2	104	0.9967
	307	0.59	0.61	3.0	7.2	0.28	2.4	0.066	85	1.32	37	1.38	4.2	12.7	85	0.9987
	305	0.56	0.57	2.9	6.6	0.30	2.3	0.066	78	1.73	49	1.70	3.4	10.2	78	0.9989
	303	0.54	0.55	2.8	6.1	0.33	2.2	0.066	69	2.7	76	2.0	2.9	8.6	69	0.9991
	302	0.52	0.64	2.7	5.8	0.35	2.1	0.066	64	3.9	110	2.3	2.5	7.6	64	0.9992
	300	0.50	0.51	2.6	5.2	0.38	2.0	0.066	11.0	57	-	-	2.9	2.0	6.0	0.9993
<i>n</i> =53.9 pcs <i>F</i> =400 sm ²																
4	310	0.62	0.52	2.6	10.2	0.20	3.9	0.037	16.6	168	1.22	30	1.0	4.0	12.0	0.9988
	307	0.59	0.48	2.4	8.8	0.23	3.7	0.037	16.3	143	1.54	38	1.38	2.9	8.7	0.9991
	305	0.56	0.46	2.3	7.9	0.25	3.5	0.037	16.1	128	2.0	49	1.74	2.3	7.0	0.9993
	303	0.54	0.44	2.2	7.3	0.28	3.3	0.037	15.7	119	3.1	76	2.0	1.98	6.0	0.9994
	302	0.52	0.43	2.15	6.9	0.29	3.2	0.037	15.4	107	4.5	109	2.3	1.73	5.2	0.9994
	300	0.50	0.40	2.0	6.2	0.32	3.0	0.037	15.3	95	-	-	2.9	1.4	4.1	0.9995

Source: compiled by the authors

With decreasing temperature at the heat-absorbing junction of the SETM TEC of a given design between the heat sink and the medium ($T - T_c$) at a given cooling temperature level $T_0 = 260K$, medium temperature $T_c = 300K$ thermal load $Q_0 = 2.0W$ geometry of the thermocouple branches (ratio $\frac{l}{S}$) for various characteristic current operating modes:

– relative operating current B decreases (Fig. 1) for different characteristic current operating modes. The relative operating current B decreases from mode Q_{0max} to mode λ_{min} at a fixed temperature at the heat-generating junction of the fuel cell or heat sink. Minimum relative operating current B_{min} . Provided in the mode λ_{min} ;

– the value of operating current I decreases (Fig. 2) for different characteristic current operating modes. The value of operating current I decreases from mode Q_{0max} to mode λ_{min} at a fixed temperature T at the heat sink or heat sink junction. The minimum value of operating current I_{min} ;

– the refrigeration coefficient E increases (Fig. 3) for different characteristic current operating modes. The maximum refrigeration coefficient E_{max} is provided in mode $(nI \lambda/\lambda_0 \tau)_{min}$;

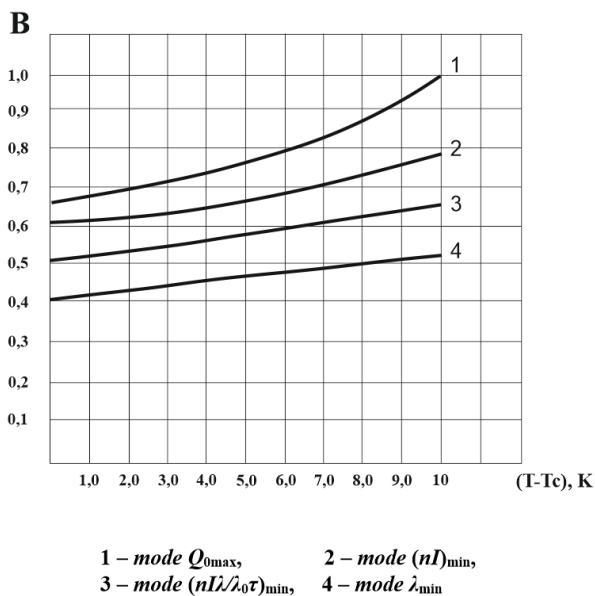


Fig. 1. Dependence of the relative operating current of the single-stage TEC on the temperature $(T - T_c)$ difference for different current operating modes at $T_0=260K$,

$T_c=300K, Q_0=2.0 W, l/S=10$

Source: compiled by the authors

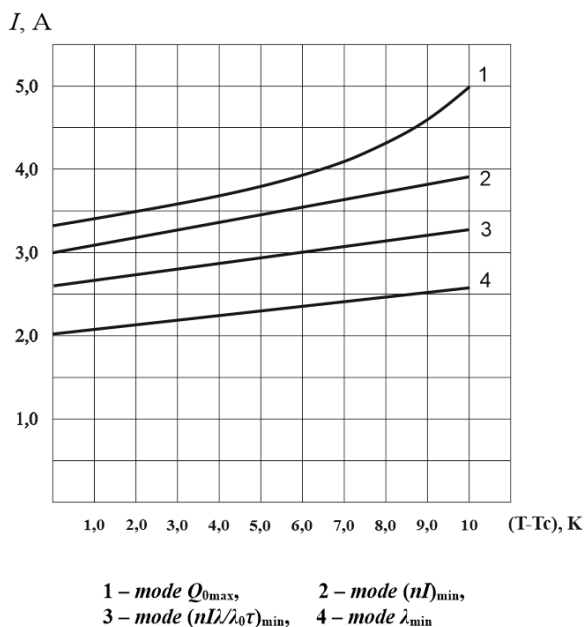


Fig. 2. Dependence of the operating current I of a single-cascade TEC on the temperature difference $(T - T_c)$ for various characteristic current operating modes at $T_0=260K, T_c=300K$,

$Q_0=2.0 W, l/S=10$

Source: compiled by the authors

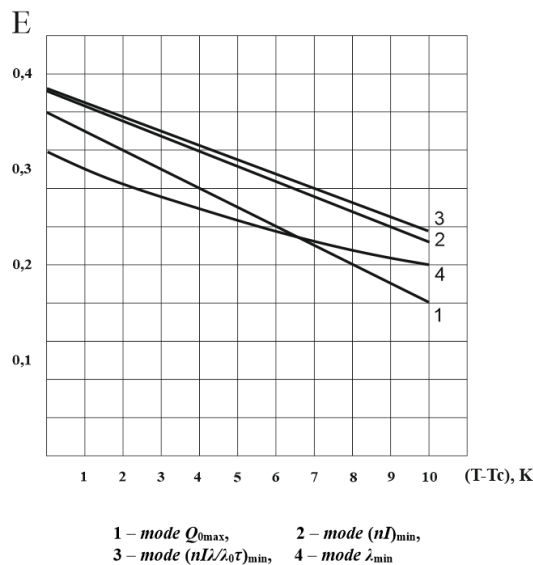


Fig.3. Dependence of the refrigeration coefficient E of a single-cascade TEC on the temperature difference $(T - T_c)$ for different characteristic current operating modes at $T_0=260K, T_c=300K$,

$Q_0=2.0 W, l/S=10$

Source: compiled by the authors

– decreases the voltage drop U (Fig. 4) for different characteristic current operating modes. Voltage drop U from the mode Q_{0max} to the mode λ_{min} at a fixed temperature T on the fuel cell junction. The maximum voltage drop U_{max} is provided in the mode λ_{min} ;

– the relative temperature drop Θ (Fig. 5) for different characteristic current operating modes decreases in the range from $\Theta = 0.62$ at $T=310K$ to $\Theta = 0.5$ at $T=300K$ (ideal heat sink);

– cooling capacity per thermocouple Q_0/n (Fig. 5) remains constant for different characteristic current operating modes. The cooling capacity per thermocouple Q_0/n increases from mode λ_{min} to mode Q_{0max} at a fixed temperature T at the heat-generating junction of the fuel cell. The maximum cooling capacity per thermocouple $(Q_0/n)_{max}$ is provided in the mode Q_{0max} ;

– decreases insignificantly the time to steady-state operation τ (Fig. 6) for different characteristic current operating modes. The time to steady-state operation τ decreases from mode λ_{min} to mode Q_{0max} at a fixed temperature T at the fuel cell junction. The minimum time to steady-state operation τ_{min} is provided in the mode Q_{0max} ;

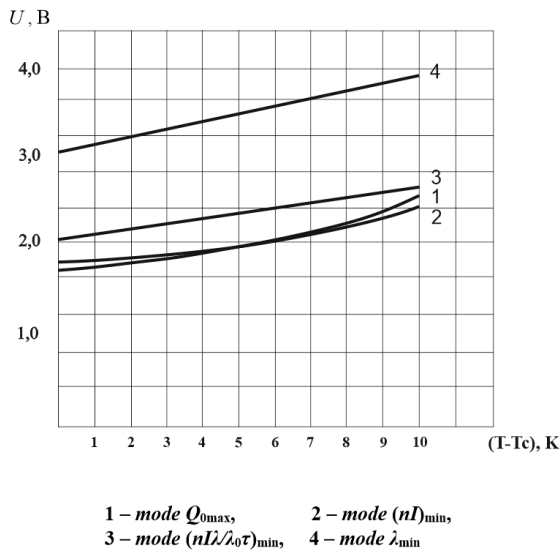


Fig. 4. Dependence of the voltage drop U of a single-stage TEC on the temperature difference $(T - T_c)$ for different current modes of operation at $T_0=260K$, $T_c=300K$, $T_c=2.0 W$,

$$I/S = 10, F = \text{const}$$

Source: compiled by the authors

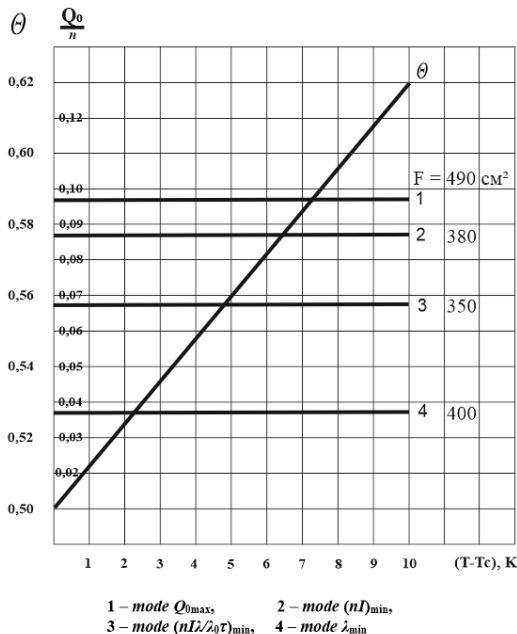


Fig. 5. Dependence of relative temperature difference and cooling capacity per one thermocouple Q_0/n of a single-cascade fuel cell on temperature difference $(T - T_c)$ for different current operating modes at $T_0=260K$, $T_c=300K$,

$$Q_0=2.0 W, I/S = 10, F = \text{const}$$

Source: compiled by the authors

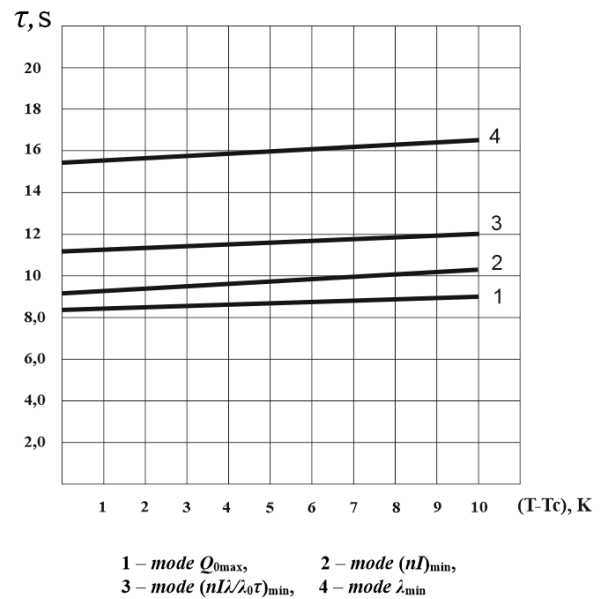


Fig. 6. Dependence of time to steady-state operation τ of a single-cascade TEC on temperature difference $(T - T_c)$ for different characteristic current operating modes at $T_0=260K$, $T_c=300K$, $T_c=2.0 W$, $Q_0=10$, $I/S = 10$

Source: compiled by the authors

– decreases the amount of expended energy N (Fig. 7) for different characteristic current operating modes. The amount of expended energy N decreases from mode λ_{min} to mode $(nI)_{min}$ at a fixed temperature T at the heat-generating junction of the fuel cell. The minimum amount of expended energy N_{min} in the mode λ_{min} ;

– the relative failure rate λ/λ_0 decreases (Fig. 8) for different characteristic current operating modes. The relative failure rate λ/λ_0 decreases from mode Q_{0max} to mode λ_{min} at a fixed temperature T at the fuel junction of the fuel cell. The minimum relative failure rate $(\lambda/\lambda_0)_{min}$ is provided in the mode λ_{min} ;

– the probability of failure-free operation P increases (Fig. 9) for different characteristic current operating modes. The probability of failure-free operation P increases from mode Q_{0max} to mode λ_{min} at a fixed temperature T at the heat sink junction of the fuel cell. The maximum probability of failure-free operation P_{max} is provided in the mode λ_{min} ;

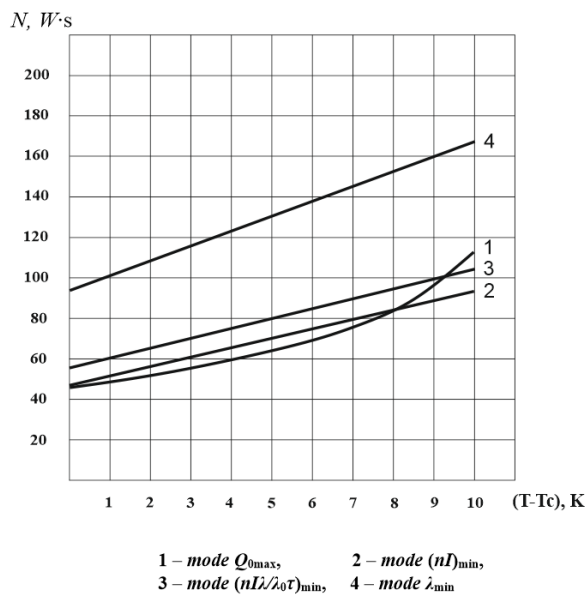


Fig. 7. Dependence of the amount of expended energy N of a single-stage TEC on the temperature $(T - T_c)$ difference for different characteristic current operating modes at $T_0=260K$, $T_c=300K$, $Q_0=2.0 W$, $l/S=10$
 Source: compiled by the authors

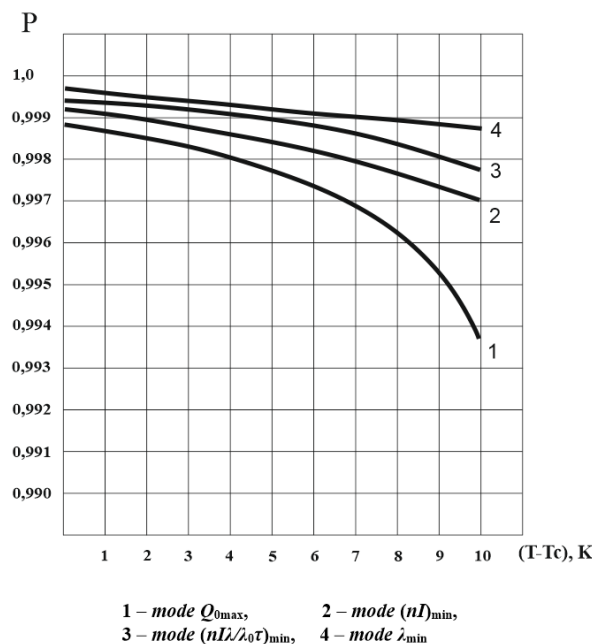


Fig. 9. Dependence of probability of failure-free operation P of a single-cascade TEC on temperature difference $(T - T_c)$ for different characteristic current operating modes at $T_0=260K$, $T_c=300K$, $Q_0=2.0 W$, $l/S=10$, $t=10^4 h$
 Source: compiled by the authors

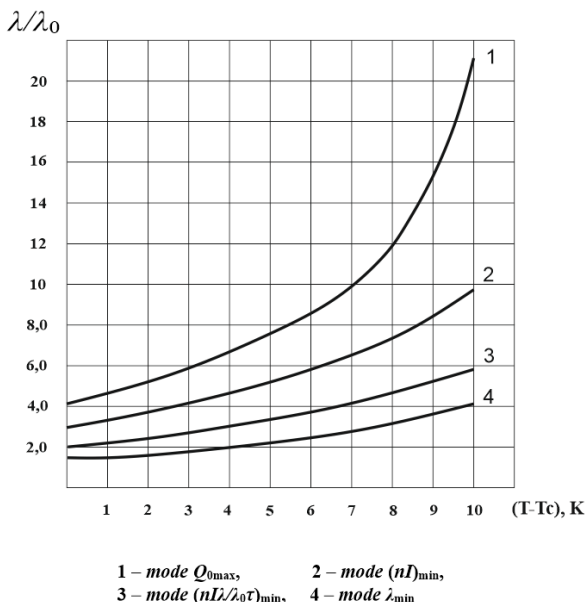


Fig. 8. Dependence of relative intensity of failures λ/λ_0 of a single-cascade TEC on temperature difference $(T - T_c)$ for different characteristic current operating modes at $T_0=260K$, $T_c=300K$, $Q_0=2.0 W$, $l/S=10$, $\lambda_0=3 \cdot 10^{-8} 1/h$
 Source: compiled by the authors

– the heat sink heat dissipation capacity αF increases (Fig. 10) for different characteristic current operating modes. The required heat sink heat dissipation capacity αF decreases from the maximum cooling capacity mode to the $(nI \lambda/\lambda_0 \tau)_{min}$.

When selecting a heat sink system consisting of a heat sink and an electric fan, it is necessary to take into account the size and mass characteristics of the system when using a ribbed radiator - variations in the height and thickness of the fin, and should also take into account the main characteristics of the electric fan: flow rate, head, type of power supply, mode of operation. As it is difficult to determine the required flow rate G (0.01–0.10)m/s accurately due to the discreteness of a number of fans, it is necessary to carry out a number of calculations for different values of velocities V (1–15)m/s.

Fig. 11 shows the dependence of the temperature drop $(T - T_c)$ at the single-stage TEC on the heat transfer coefficient α at the heat sink with surface area F for various characteristic current operating modes. As the heat transfer coefficient α

increases, the temperature drop $(T - T_c)$ decreases at a fixed heat sink surface area F .

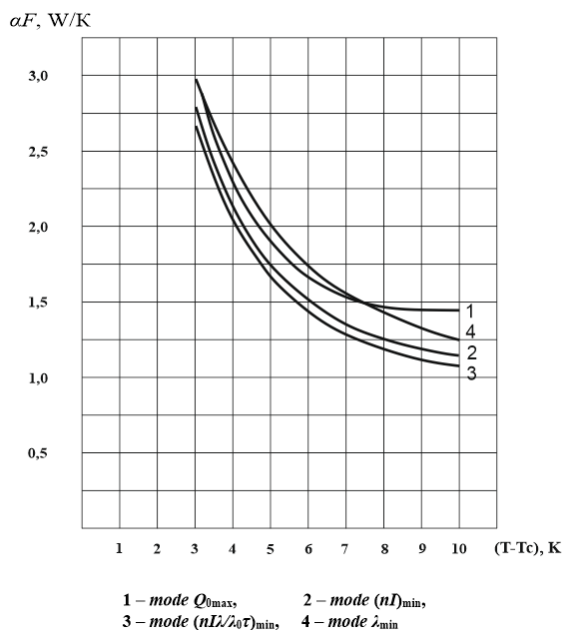


Рис. 10. Зависимость теплоотводящей способности радиатора αF однокаскадного ТЭУ от перепада температур $(T - T_c)$ для различных характерных токовых режимов работы при $T_0=260K$, $T_c=300K$, $Q_0=2.0 W$

Source: compiled by the authors

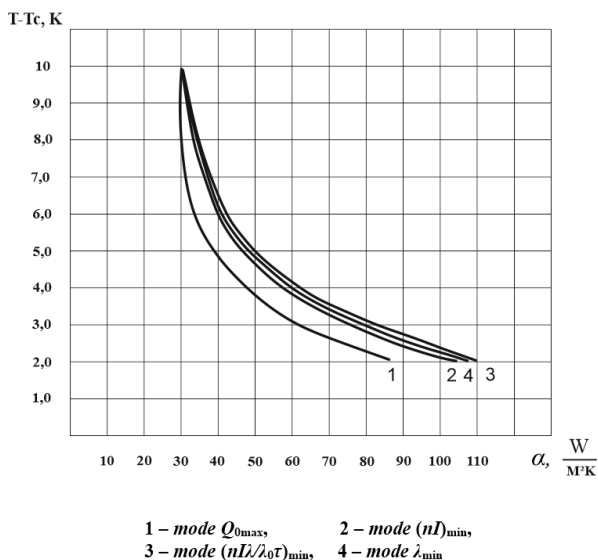


Fig. 11. Dependence of the temperature drop $(T - T_c)$ on a single-cascade TEC on the heat transfer coefficient α of the heat sink for various characteristic current operating modes

$T_0=260K$, $T_c=300K$, $Q_0=2.0 W$

Source: compiled by the authors

Fig. 12 shows the dependence of the required heat dissipation capacity of the heat sink αF of a single-stage TEC on the heat dissipation coefficient α for various characteristic current operating modes.

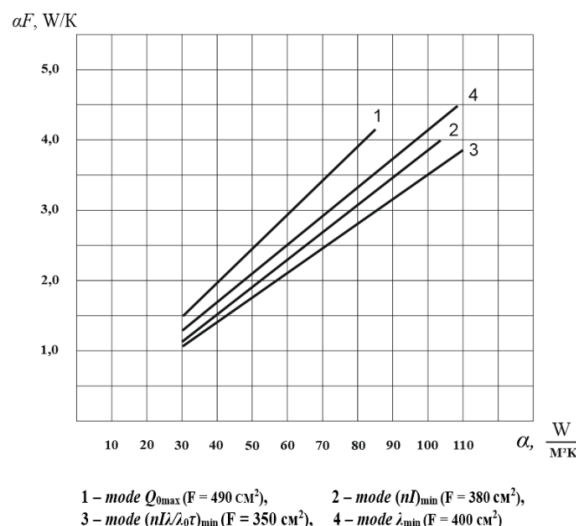


Fig. 12. Dependence of the required heat dissipation capacity αF of the heat sink of a single-stage TEC on the heat dissipation coefficient α for various characteristic current operating modes at

$T_0=260K$, $T_c=300K$, $Q_0=2.0 W$

Source: compiled by the authors

As the heat transfer coefficient increases, the heat dissipation capacity of the heat sink αF increases for different operating modes at a fixed heat sink surface area F . The minimum heat dissipation capacity of the heat sink αF_{min} is provided in the mode $(nI/\lambda_0\tau)_{min}$.

ANALYSIS OF THE MODEL

The analysis of research results showed that with decreasing temperature difference $(T - T_c)$ at $T_0=260K$, $T_c=300K$, $Q_0=2.0W$, $l/S=10$:

– the ratio $K = \frac{\lambda^{(T-T_c)=10K}}{\lambda^{(T-T_c)=Var}}$ of relative failure rate λ/λ_0 at $(T - T_c)=10K$ set to relative failure rate at $(T - T_c)=Var < 10K$ increases (Fig. 13) for different characteristic current operating modes.

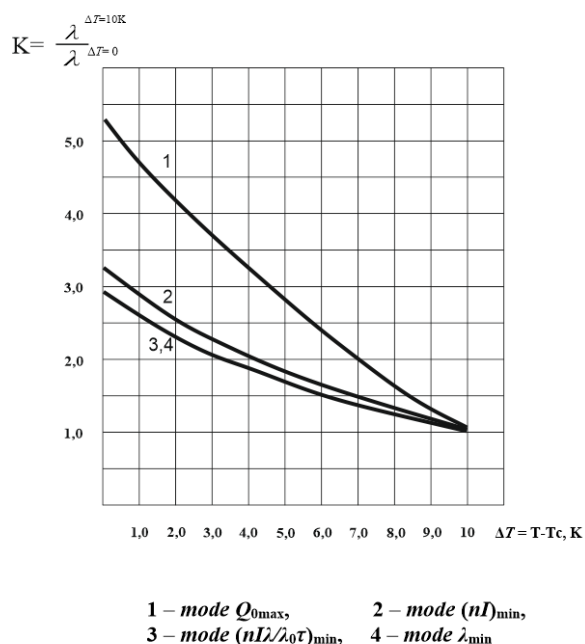


Fig. 13. Dependence of the ratio $K = \frac{\lambda^{(T-T_c)=10K}}{\lambda^{(T-T_c)=Var}}$

of a single-stage TEC on the temperature difference $(T - T_c)$ for different characteristic current operating modes at

$T_0=260K, T_c=300K, Q_0=2.0 W$

Source: compiled by the authors

Thus, for the operating mode $Q_{0\max}$:

at $(T - T_c) = 10K$ $K=1.0$;

at $(T - T_c) = 7K$ $K=2.0$, i.e. relative intensity of failures λ/λ_0 decreases in 2 times;

at $(T - T_c) = 5K$ $K=2.8$, i.e. decreases in 2.8 times;

at $(T - T_c) = 3K$ $K=3.5$, i.e. it decreases by 3.5 times;

at $(T - T_c) = 2K$ $K=4.0$, i.e. decreases by 4.0 times.

For the mode $(nI)_{\min}$:

at $(T - T_c) = 10K$ $K=1.0$;

at $(T - T_c) = 7K$ $K=1.5$, i.e. decreases by 1.5 times;

at $(T - T_c) = 5K$ $K=1.8$, i.e. decreases by a factor of 1.8 times;

at $(T - T_c) = 3K$ $K=2.3$, i.e. decreases by a factor of 2.3 times;

at $(T - T_c) = 2K$ $K=2.5$, i.e. decreases by 2.5 times.

For the regime $(nI/\lambda_0\tau)_{\min}$ and λ_{\min} :

at $(T - T_c) = 10K$ $K=1.0$;

at $(T - T_c) = 7K$ $K=1.3$, i.e. decreases by 30%;

at $(T - T_c) = 5K$ $K=1.7$, i.e. decreases by 70%;

at $(T - T_c) = 3K$ $K=2.1$, i.e. decreases by 2.1 times;

at $(T - T_c) = 2K$ $K=2.3$, i.e. decreases by 2.3 times.

Consequently, the probability of failure-free operation P increases:

for operating mode $Q_{0\max}$:

from $P=0.9937$ at $(T - T_c) = 10K$ to $P=0.9985$ at $(T - T_c) = 2K$;

for operation mode $(nI)_{\min}$:

from $P=0.9971$ at $(T - T_c) = 10K$ to $P=0.9989$ at $(T - T_c) = 2K$;

for operating mode $(nI/\lambda_0\tau)_{\min}$:

$P=0.9967$ at $(T - T_c) = 10K$ to $P=0.99924$ at $(T - T_c) = 2K$;

for operating mode λ_{\min} :

$P=0.9988$ at $(T - T_c) = 10K$ to $P=0.99948$ at $(T - T_c) = 2K$.

Thus decreases:

– relative temperature difference Θ from $\Theta = 0.62$ at $(T - T_c) = 10K$ to $\Theta = 0.525$ at $(T - T_c) = 2K$, i.e. by 15% for all characteristic operating modes;

– relative operating current B :

for mode $Q_{0\max}$:

from $B = 1.0$ at $(T - T_c) = 10K$ to $B=0.70$ at $(T - T_c) = 2K$, i.e. by 30%;

for mode $(nI)_{\min}$:

from $B=0.79$ at $(T - T_c) = 10K$ to $B=0.63$ at $(T - T_c) = 2K$, i.e. by 20%;

for mode $(nI/\lambda_0\tau)_{\min}$:

from $B=0.65$ at $(T - T_c) = 10K$ to $B=0.54$ at $(T - T_c) = 2K$, i.e. by 17%;

for mode λ_{\min} :

from $B=0.52$ at $(T - T_c) = 10K$ to $B=0.43$ at $(T - T_c) = 2K$, i.e. by 17%;

– is the value of the operating current I :

for mode $Q_{0\max}$:

from $I=5.0A$ at $(T - T_c) = 10K$ to $I=3.5A$ at $(T - T_c) = 2K$, i.e. by 30%;

for mode $(nI)_{\min}$:

from $I=3.9\text{A}$ at $(T-T_c)=10\text{K}$ to $I=3.17\text{A}$ at $(T-T_c)=2\text{K}$, i.e. by 19%;

for mode $(nI \lambda / \lambda_0 \tau)_{\min}$:

from $I=3.3\text{A}$ at $(T-T_c)=10\text{K}$ to $I=2.7\text{A}$ at $(T-T_c)=2\text{K}$, i.e. by 18%;

for mode λ_{\min} :

from $I=2.6\text{A}$ at $(T-T_c)=10\text{K}$ to $I=2.15\text{A}$ at $(T-T_c)=2\text{K}$, i.e. by 17 %;

– voltage drop U :

for the mode $Q_{0\max}$:

from $U=2.5\text{V}$ at $(T-T_c)=10\text{K}$ to $U=1.8\text{V}$ at $(T-T_c)=2\text{K}$, i.e. by 28 %;

for mode $(nI)_{\min}$:

from $U=2.4\text{V}$ at $(T-T_c)=10\text{K}$ to $U=1.86\text{A}$ at $(T-T_c)=2\text{K}$, i.e. by 19 %;

for mode $(nI \lambda / \lambda_0 \tau)_{\min}$:

from $U=2.6\text{V}$ at $(T-T_c)=10\text{K}$ to $U=2.1\text{V}$ at $(T-T_c)=2\text{K}$, i.e., by 19 %;

for mode λ_{\min} :

from $U=3.9\text{A}$ at $(T-T_c)=10\text{K}$ to $U=3.2\text{V}$ at $(T-T_c)=2\text{K}$, i.e. by 18 %;

– time to reach steady-state operation τ :

for mode $Q_{0\max}$:

from $\tau=9.0\text{s}$ at $(T-T_c)=10\text{K}$ to $\tau=8.6\text{s}$ at $(T-T_c)=2\text{K}$, i.e. by 4.4%;

for mode $(nI)_{\min}$:

from $\tau=10.2\text{s}$ at $(T-T_c)=10\text{K}$ to $\tau=9.4\text{s}$ at $(T-T_c)=2\text{K}$, i.e. by 7.8%;

for mode $(nI \lambda / \lambda_0 \tau)_{\min}$:

from $\tau=12.1\text{s}$ at $(T-T_c)=10\text{K}$ to $\tau=11.1\text{s}$ at $(T-T_c)=2\text{K}$, i.e. by 8.3%;

for mode λ_{\min} :

from $\tau=16.6\text{s}$ at $(T-T_c)=10\text{K}$ to $\tau=15.4\text{s}$ at $(T-T_c)=2\text{K}$, i.e. by 7.2%;

– amount of energy consumed N :

for the mode $Q_{0\max}$:

from $N=113\text{Ws}$ at $(T-T_c)=10\text{K}$ to $N=54\text{Ws}$ at $(T-T_c)=2\text{K}$, i.e. 2.1 times;

for the mode $(nI)_{\min}$:

from $N=95\text{Ws}$ at $(T-T_c)=10\text{K}$ to $N=56\text{Ws}$ at $(T-T_c)=2\text{K}$, i.e., by a factor of 1.7;

for mode $(nI \lambda / \lambda_0 \tau)_{\min}$:

from $N=104\text{Ws}$ at $(T-T_c)=10\text{K}$ to $N=64\text{Ws}$ at $(T-T_c)=2\text{K}$, i.e., by a factor of 1.6;

for mode λ_{\min} :

from $N=168\text{Ws}$ at $(T-T_c)=10\text{K}$ to $N=107\text{Ws}$ at $(T-T_c)=2\text{K}$, i.e., by a factor of 1.57;

– increases the refrigeration coefficient E :

for the mode $Q_{0\max}$:

from $E=0.16$ at $(T-T_c)=10\text{K}$ to $E=0.32$ at $(T-T_c)=2\text{K}$, i.e. by a factor of 2.0;

for the mode $Q_{0\max}$:

from $E=0.22$ at $(T-T_c)=10\text{K}$ to $E=0.34$ at $(T-T_c)=2\text{K}$, i.e. by 55%;

for mode $(nI \lambda / \lambda_0 \tau)_{\min}$:

from $E=0.23$ at $(T-T_c)=10\text{K}$ to $E=0.35$ at $(T-T_c)=2\text{K}$, i.e. by 52%;

for mode λ_{\min} :

from $E=0.20$ at $(T-T_c)=10\text{K}$ to $E=0.29$ at $(T-T_c)=2\text{K}$, i.e. by 45%;

– increases heat dissipation capacity αF :

for mode $Q_{0\max}$:

from $\alpha F=1.46\text{W/K}$ at $(T-T_c)=10\text{K}$ to $\alpha F=4.15\text{W/K}$ at $(T-T_c)=2\text{K}$, i.e. 2.8 times;

for mode $(nI)_{\min}$:

from $\alpha F=1.13\text{W/K}$ at $(T-T_c)=10\text{K}$ to $\alpha F=4.0\text{W/K}$ at $(T-T_c)=2\text{K}$, i.e. by a factor of 3.5;

for mode $(nI \lambda / \lambda_0 \tau)_{\min}$:

from $\alpha F=1.06\text{W/K}$ at $(T-T_c)=10\text{K}$ to $\alpha F=3.3\text{W/K}$ at $(T-T_c)=2\text{K}$, i.e., by a factor of 3.7;

for mode λ_{\min} :

from $\alpha F=1.22\text{W/K}$ at $(T-T_c)=10\text{K}$ to $\alpha F=4.5\text{W/K}$ at $(T-T_c)=2\text{K}$, i.e. by a factor of 3.7.

At the same time, the cooling capacity per thermocouple Q_0/n remains constant for each characteristic current mode of operation.

CONCLUSIONS

The mathematical model of SETM (object – heat sink – heat dissipating radiator - fan) has been developed to estimate the influence of conditions of heat exchange of heat sink with medium on the main parameters, reliability indicators, dynamics and energy characteristics of a single-cascade TEC at a given temperature level of cooling T_0 , medium temperature T_c , geometry of branches of thermoelements (ratio l/S) for various characteristic current operating modes.

The analysis of the research results has shown the possibility of:

– the relative intensity λ/λ_0 of failures from 2.3 to 4.0 times decreases; the values of operating

current I from 17 % to 30 %; the time of exit to the stationary mode of operation τ from 4.4 % to 8.0%; the amount of expended energy N from 1.6 to 2.1 times;

– cooling coefficient E increases from 45% to 2.0 times; probability of failure-free operation P from $P=0.9985$ to $P=0.99948$ for various characteristic current operating modes.

Thus, the reduction of temperature difference $(T-T_c)$ in the system of SETM allows to reduce considerably the relative intensity of failures, and, consequently, to increase the probability of failure-free operation λ/λ_0 of the fuel and power unit and thus to control the reliability indicators of the SETM system of a given design.

REFERENCES

1. Borshchev, N. O., Belyavskiy, A. O. & Antonov, V. A. “Analysis of the systems for thermal modes of domestic spacecrafts”. *Engineering Journal: Science and Innovations*. 2022; 7: 1–19. DOI: <https://doi.org/10.18698/2308-6033-2022-7-2193>.
2. Cai, Y., Hong, B.-H., Wu, W.-X., Wang, W.-W. & Zhao, F.-Y. “Active cooling performance of a PCM-based thermoelectric device: Dynamic characteristics and parametric investigations”. *Energy*. 2022; 254: 124356. DOI: <https://doi.org/10.1016/j.energy.2022.124356>.
3. Tang, J., Ni, H., Peng, R.-L., Wang, N. & Zuo, L. J. J. “A review on energy conversion using hybrid photovoltaic and thermoelectric systems”. *Journal of Power Sources*. 2023; 562: 232785. DOI: <https://doi.org/10.1016/j.jpowsour.2023.232785>.
4. Arranz, M. C., Birk, W. & Kadhim, A. “On guided and automatic control configuration selection”. *22nd IEEE International Conference on Emerging Technologies and Factory Automation (ETFA)*. 2017. p. 1–6. DOI: <https://doi.org/10.1109/ETFA.2017.8247700>.
5. Stopakevych, A. & Stopakevych, O. “Analytical review of distillation columns decentralized control systems design methods”. *Informatics and Mathematical Methods in Simulation*. 2021; 11 (4): 343–357. DOI: <https://doi.org/10.15276/imms.v11.no4.343>.
6. Xie, S., Zeng, Y., Qian, J., Yang, F. & Li, Y. “CPSOGSA optimization algorithm driven cascaded 3DOF-FOPID-FOPID controller for load frequency control of DFIG-containing interconnected power system”. *Energies*. 2023; 16: 1364. DOI: <https://doi.org/10.3390/en16031364>.
7. Memon, S. & Kalhor, A. N. “Design of multivariable PID controllers: A comparative study”. *IJCSNS International Journal of Computer Science and Network Security*. 2021; 21 (8): 377–384. DOI: <https://doi.org/10.22937/IJCSNS.2021.21.8.47>.
8. Gorskyi, P. V. “Particular aspects of determining reliability indicators of thermoelectric generator modules using experimental data”. *Tekhnologiya i Konstruirovaniye v Elektronnoi Apparature*. 2022; 1–3: 50–56. DOI: <https://doi.org/10.15222/TKEA2022.1-3.50>.
9. Shilpa, M. K., Raheman, M. A., Aabid, A. & Baig, M. “A systematic review of thermoelectric peltier devices: Applications and limitations”. *Fluid Dynamics and Materials Processing*. 2022; 19 (1): 187–206. DOI: <https://doi.org/10.32604/fdmp.2022.020351>.
10. Patil, N.G. & Hotta, T. K. “Combined liquid cold plate and heat sink based hybrid cooling approach for the temperature control of integrated circuit chips”. *ASME*. 2022; 14: 111013. DOI: <https://doi.org/10.1115/1.4054849>.

11. Ebale, L. O., Pierre Gomat, L. J., Nzonzolo, L., Mavoungou, M. R. & Kibongani, F. “Optimization of a thermoelectric cooling system with Peltier Effect”. *Am. J. Energ. Eng.* 2019; 7(3): 55–63. DOI: <https://doi.org/10.11648/j.sjee.20190703.12>.
12. Venkatesan, K. & Venkataramanan, M. “Experimental and simulation studies on thermoelectric cooler: A performance study approach”. *International Journal of Thermophysics.* 2020; 41 (4): 38. DOI: <https://doi.org/10.1007/s10765-020-2613-2>.
13. Lu, T., Li, Y., Zhang, J., Ning, P. & Niu, P. “Cooling and mechanical performance analysis of a trapezoidal thermoelectric cooler with variable cross-section”. *Energies.* 2020; 13: 6070. DOI: <https://doi.org/10.3390/en13226070>.
14. Shi, X.-L., Zou, J. & Chen, Z.-G. “Advanced thermoelectric design: from materials and structures to devices”. *Chem. Rev.* 2020; 120: 7399–7515. DOI: <https://doi.org/10.1021/acs.chemrev.0c00026>.
15. Zhang, J., Huadong, Z., Feng, B., Song, X., Zhang, X. & Zhang, R. “Numerical simulations and optimized design on the performance and thermal stress of a thermoelectric cooler”. *International Journal of Refrigeration.* 2022; 146: 314–326. DOI: <https://doi.org/10.1016/j.ijrefrig.2022.11.010>.
16. Wu, Y., Zhang, P., Chen, S., Zhi, C., Shi, T., Gong, T. & Ming, T. “Performance optimization of the transient thermoelectric cooling for the temperature control of the chip working under dynamic power”. *Case Studies in Thermal Engineering.* 2024; 58: 104350. DOI: <https://doi.org/10.1016/j.csite.2024.104350>.
17. Zaykov, V. P., Mescheryakov, V. I. & Zhuravlov, Yu. I. “Analysis of dynamic and reliability indicators of a thermoelectric cooler at minimization of a complex of three basic parameters”. *Herald of Advanced Information Technology.* 2020; 3 (3): 174–184. DOI: <https://doi.org/10.15276/hait.03.2020.6>.
18. Zaykov, V. P., Mescheryakov, V. I. & Ustenko, A. I. “Method of reliability control of thermoelectric systems to ensure thermal regimes”. *Herald of Advanced Information Technology.* 2024; 7 (1): 58–69. DOI: <https://doi.org/10.15276/hait.07.2024.5>.

Conflicts of Interest: the authors declare no conflict of interest

Received 05.08.2024

Received after revision 14.09.2024

Accepted 20.09.2024

DOI: <https://doi.org/10.15276/hait.07.2024.22>

УДК 004.662.99·519.6

Контроль якості функціонування структури “об’єкт-термоелектричний охолоджувач-тепловідвідний радіатор” системи забезпечення теплових режимів

Зайков Володимир Петрович¹

ORCID: <https://orcid.org/0000-0002-4078-3519>; gradan@i.ua. Scopus Author ID: 57192640250

Мещеряков Володимир Іванович²

ORCID: <https://orcid.org/0000-0003-0499-827X>; gradan@ua.fm. Scopus Author ID: 57192640885

Устенко Андрій Сергійович²

ORCID: <https://orcid.org/http://orcid.org/0000-0002-0546-7019>; uas059877@gmail.com

Тройніна Анастасія Сергіївна³

ORCID: <https://orcid.org/0000-0001-6862-1266>; anastasiyatroynina@gmail.com. Scopus Author ID: 57193992712

¹ Науково-дослідницький інститут ШТОПМ, вул. Терешкової 27. Одеса, 65076, Україна

² Одеський національний університет ім. Мечникова, вул. Дворянська, 2. Одеса, 65082, Україна

³ Одеський національний політехнічний університет, пр. Шевченка, 1. Одеса, 65044, Україна

АНОТАЦІЯ

Розглянуто аналіз математичної моделі системи забезпечення теплових режимів з використанням термоелектричного охолодження для оцінювання впливу умов теплообміну тепловідвідного радіатора із середовищем на основні параметри, показники надійності та динамічні характеристики однокаскадного термоелектричного охолоджувача за заданого температурного рівня охолодження, температури середовища, геометрії гілок термоелементів для різних струмових режимів роботи. Наведено результати розрахунків основних значущих параметрів, показників надійності, динамічних та енергетичних характеристик однокаскадного охолоджувача і тепловідвідного радіатора обраної конструкції при заданому температурному рівні охолодження, температурі середовища, тепловому навантаженні, геометрії гілок термоелементів для різних характерних струмових режимів роботи за умови зміни умов теплообміну на тепловідвідному радіаторі заданої конструкції при варіації коефіцієнта тепловіддачі. Показано, що зі збільшенням швидкості потоку повітря на тепловідвідному радіаторі збільшується коефіцієнт тепловіддачі й у такий спосіб зменшується перепад температур на тепловідвідному спай термоелектричного охолоджувача із середовищем, що дає змогу значно зменшити відносну інтенсивність відмов охолоджувача й у такий спосіб підвищити ймовірність безвідмовної роботи всього пристрою. Під час функціонування системи забезпечення теплових режимів, що складається з охолоджувального пристрою, тепловідвідного радіатора, електровентилятора, застосовуваного для відведення теплової потужності в навколишнє середовище, можна використовувати різні режими роботи електровентилятора (витрата повітря). Зі зростанням витрати повітря електровентилятором збільшується швидкість потоку повітря в живому перерізі тепловідвідного радіатора заданої конструкції, що призводить до зростання коефіцієнта тепловіддачі. Це, своєю чергою, дає змогу зменшити перепад температури за заданої конструкції системи забезпечення теплових режимів. Розглянуто можливість керування показниками надійності, а саме, відносною інтенсивністю відмов і ймовірністю безвідмовної роботи систем забезпечення теплових режимів різних конструкцій (струмові режими, кількість термоелементів, площа поверхні радіатора) за заданого рівня охолодження (температура середовища, теплове навантаження, геометрія термоелементів) у разі зміни умов теплообміну тепловідвідного радіатора із середовищем.

Ключові слова: показники надійності; динамічні характеристики; маса та габарити; перепад температур; струмовий режим

ABOUT THE AUTHORS



Vladimir P. Zaykov - PhD (Eng), Head of Sector Research Institute "STORM", 27, Tereshkova Str. Odessa, 65076, Ukraine

ORCID: <https://orcid.org/0000-0002-4078-3519>; gradan@i.ua. Scopus Author ID: 57192640250

Research field: Reliability and dynamic descriptions of thermo-electric cooling devices; design, planning of the systems of providing of the thermal modes of electronic apparatus

Зайков Володимир Петрович - кандидат технічних наук, начальник сектору науково – дослідного інституту «ШТОРМ», вул. Терешкової 27. Одеса, 65076, Україна



Vladimir I. Mescheryakov - Doctor of Engineering Sciences, Professor, Head of Department of Informatics, Odessa Mechnikov National University, 2, Dvoryanska Str. Odessa, 65082, Ukraine.

ORCID: <http://orcid.org/0000-0003-0499-827X>; gradan@ua.fm. Scopus Author ID: 57192640885

Research field: Reliability and dynamic descriptions of thermo-electric cooling devices; design of power biotechnical informative systems

Мещеряков Володимир Іванович - доктор технічних наук, зав. кафедри Інформатики. Одеський національний університет ім. Мечникова, вул. Дворянська, 2. Одеса, 65082, Україна



Andrii S. Ustenko - Graduate Student. Odessa Mechnikov National University, 2, Dvoryanska Str. Odessa, 65082, Ukraine.

ORCID: 0000-0002-0546-7019; uas059877@gmail.com

Research field: Reliability and dynamic descriptions of thermo-electric cooling devices; planning of the systems of providing of the thermal modes of electronic apparatus

Устенко Андрій Сергійович - аспірант. Одеський національний університет ім. Мечникова, вул. Дворянська, 2. Одеса, 65082, Україна



Anastasiya S. Troynina - Candidate of Engineering Science, Associate Professor, Department of Software Engineering, Odessa National Polytechnic University, 1, Shevchenko Ave. Odessa, 65044, Ukraine

ORCID: <https://orcid.org/0000-0001-6862-1266>; anastasiyatroynina@gmail.com. Scopus Author ID: 57193992712

Research field: Big data, data mining, artificial intelligence, knowledge based

Тройніна Анастасія Сергіївна - кандидат технічних наук, доцент кафедри Інженерії програмного забезпечення. Одеський національний політехнічний університет, пр. Шевченка, 1. Одеса, 65044, Україна